Pulsed Nuclear Magnetic Resonance: Spin Echoes

Sara L. Campbell and Javier M. G. Duarte*
MIT Department of Physics
(Dated: Wednesday, October 29, 2008)

Pulsed nuclear magnetic resonance (NMR) techniques were used to find nuclear magnetic moments of hydrogen and fluorine as well as the spin-lattice relaxation time T_1 and the spin-spin relaxation time T_2 for different viscosities of glycerine. The nuclear magnetic moment of hydrogen was found to be $(1.4099 \pm .0048) * 10^{-26}$ Joules/Tesla and the nuclear magnetic moment of fluorine was found to be $(1.4094 \pm 0.0056) * 10^{-26}$ Joules/Tesla. T_1 values were found using a the three pulse sequence, but our data was poor. T_2 value were successfully measured using the Carr-Purcell pulse sequence and a negative linear relationship on a log-log plot of T_2 versus viscosity for different viscosities of glycerine was found. In all cases, expected free induction decay and spin echo behavior was observed.

1. INTRODUCTION

Nuclear magnetic resonance (NMR) was developed independently by Felix Bloch and Edward Purcell. In 1952 they shared the Nobel Prize for their discoveries. Nuclear magnetic resonance uses a small magnetic field oscillating at radio frequencies to excite a sample with nuclear magnetic moments that are nominally aligned with a large static electric field. NMR techniques have a wide variety of applications, including precision magnetic field measurement and magnetic resonance imaging (MRI). In this experiment, we use NMR to find the nuclear magnetic moments of hydrogen and fluorine and the spin-lattice relaxation time T_1 and the spin-spin relaxation time T_2 for different viscosities.

2. BACKGROUND AND THEORY

2.1. Classical Model of Larmor Precession

We first consider a particle with spin angular momentum $|\vec{S}| = S\hbar$ and magnetic dipole $\vec{\mu} = \gamma\vec{S}$ in a static magnetic field $\vec{B_o}$, as shown in figure 1. Bloch showed that the ensemble average of many quantum mechanical systems follows the same laws as a classical mechanical system.[1]. Our samples contain a large number of nuclei, so a classical model will be sufficient to describe this phenomenon. Letting θ be the angle between $\vec{B_0}$ and $\vec{\mu}$, we set the torque due to $\vec{B_o}$ equal to the change in angular momentum I to obtain the precession frequency w_0,

$$|\tau| = |\vec{\mu} \times \vec{B_o}| = |\gamma\vec{S} \times \vec{B_0}| = \gamma S B_0 \sin\theta \qquad (1)$$

$$|\tau| = |\frac{d\vec{S}}{dt}| = S\sin\theta\omega_0 \Rightarrow \omega_0 = \gamma B_0 \qquad (2)$$

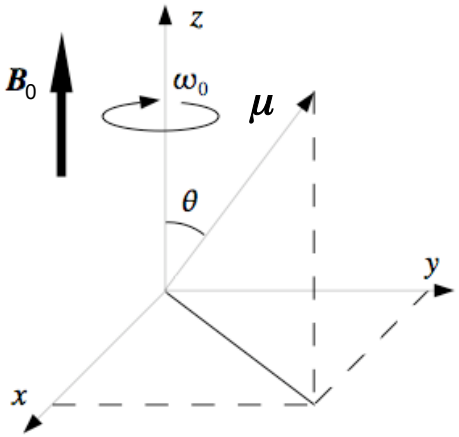

FIG. 1: Diagram of the configuration for the classical model of spin precession.

2.2. Bloch Sphere Representation

Like a bit is the basic unit of computer information, the qubit is the basic unit of quantum information. Qubit states $|\psi\rangle$ are states of a two-level quantum mechanical system with respect some observable, and can be expressed as the linear superposition of the eigenstates of the observable operator. If the two eigenstates are $|+\rangle$ and $|-\rangle$, without loss of generality we can express $|\psi\rangle$ as,

$$|\psi\rangle = \cos(\frac{\theta}{2})|-\rangle + e^{i\phi}\sin(\frac{\theta}{2})|+\rangle, \qquad (3)$$

as we require that $\langle\psi|\psi\rangle = 1$, and because we can only observe $\langle\psi|\psi\rangle$, only the difference in phase between the two components ϕ is relevant.

A wave function with a particular θ and ϕ corresponds to the point $(\cos\phi\sin\theta, \sin\phi\sin\theta, \cos\theta)$ on the unit sphere. This representation can help us visualize $|\phi\rangle$ in space.

*Electronic address: campsoup@mit.edu, woodson@mit.edu

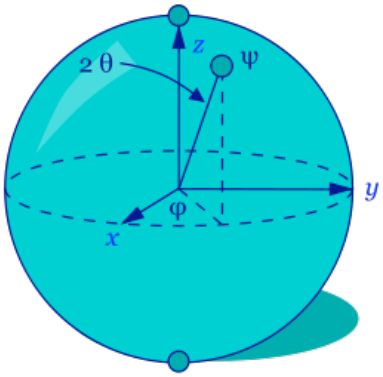

FIG. 2: Diagram of the Bloch sphere representation, illustrating how we can consider each qubit state in our sample to be a vector $(\cos\phi\sin\theta, \sin\phi\sin\theta, \cos\theta)$ on the unit sphere. Image from Wikipedia.

2.3. Quantum Mechanical Description of Nuclear Magnetic Resonance

The quantum mechanical description of a particle with spin angular momentum in a magnetic field[2] is similar to the classical description. Intead of a spin vector, we have a spin operator $\hat{S} = (\hat{S_x}, \hat{S_y}, \hat{S_z})$ that acts on the particle's wave function $|\psi\rangle$. The magnetic dipole moment is $\vec{\mu} = \gamma\hat{S}$. For nuclear magnetic resonance, we have the static magnetic field $\vec{B_o}$, and we apply an additional time-oscillating circularly polarized magnetic field $\vec{B_1}$, perpendicular to $\vec{B_0}$. In coordinates, we can express the net magnetic field and Hamiltonian $\hat{H} = \vec{\mu}\cdot\vec{B(t)}$ in the lab frame,

$$\vec{B(t)} = (B_1\cos wt, -B_1\sin wt, B_0) \tag{4}$$

$$\hat{H(t)} = -\gamma B_0\hat{S_z} - \gamma B_1(\hat{S_x}\cos\omega t - \hat{S_y}\sin\omega t) \tag{5}$$

Using the rotation operator $e^{-i\omega t\hat{S_z}/\hbar}$ we express $\hat{H(t)}$ as,

$$\hat{H(t)} = e^{i\omega t\hat{S_z}/\hbar}(-\gamma B_o\hat{S_z} - \gamma B_1\hat{S_x})e^{-i\omega t\hat{S_z}/\hbar} \tag{6}$$

Therefore, if we consider the system in the frame rotating about the z axis at angular frequency ω, the rotated Hamiltonian $\hat{H} = -\gamma B_0\hat{S_z} - \gamma B_1\hat{S_x}$ is time independent. We express the particle's wave function in the rotating frame $|\psi_{\text{rot}}\rangle$ as,

$$|\psi_{\text{rot}}\rangle = e^{-i\omega t\hat{S_z}/\hbar}|\psi(t)\rangle \tag{7}$$

Schrödinger's equation in the rotated frame becomes,

$$i\hbar\frac{d}{dt}|\psi_{\text{rot}}(t)\rangle = -\gamma\vec{B_{\text{eff}}}\cdot\hat{S}|\psi_{\text{rot}}\rangle$$

where,

$$\vec{B_{\text{eff}}} = (B_0 - \frac{\omega}{\gamma})\hat{e_z} + B_1\hat{e_x}$$

If $\omega_0 = \omega$, that is, if ω is tuned to the resonant frequency of the particle (same as the Larmor frequency calculated earlier), Schrödinger's equation becomes,

$$i\hbar\frac{d}{dt}|\psi_{\text{rot}}\rangle = -\gamma B_1\hat{S_x}|\psi_{\text{rot}}(t)\rangle$$

and we have precession in the (z, ψ_{rot}) plane with frequency γB_1. The rotated Hamiltonian is time-independent, so to calculate what happens to $|\psi_{\text{rot}}\rangle$ if we turn on B_1 at the resonant frequency for time Δt, we can simply apply the time evolution operator,

$$|\psi_{\text{rot}}(\Delta t)\rangle = e^{-i\omega_0\Delta t S_z/\hbar}|\psi_{\text{rot}}(0)\rangle$$

In this experiment we will need to rotate the ensemble average of the spins by $\pi/2$ and π degrees. We will pick pulse durations such that $\omega_0\Delta t S_z/\hbar = \gamma B_1\Delta t = \pi/2, \pi$. We refer to these as $\pi/2$ or 90^o pulses and π or 180^o pulses.

2.4. Definition of The Spin-Lattice Relaxation Time T_1 and the Spin-Spin Relaxation Time T_2

Quantum mechanically, atomic nuclei may only be in one of two spin states: up or down, written as $|+\rangle$ or $|-\rangle$. From the canonical ensemble in statistical physics, in thermal equilibrium, the probability that a given spin is in state $|+\rangle$ or $|-\rangle$ is $P(\pm) = e^{E_\pm/kT}/Z$, where $E_\pm$ is the energy associated with the two states, k is Boltzmann's constant, T is the temperature and Z is the partition function.[3] T_1 is a measure of how quickly the nuclei transfer energy to their surroundings. Once excited with a RF burst, the spin distribution will "cool' back to the original Boltzmann distribution exponentially with time constant T_1. From Stichter[4], if n_0 is the initial population difference between the excited and unexcited distributions, and $n(t)$ is the population difference at time t,

$$n(t) = n_0(1 - e^{-t/T_1}) \tag{8}$$

Whereas the spin-lattice relaxation time T_1 is the time constant associated return to the equilibrium magnetization in the longitudinal (z) direction, the spin-spin relaxation time T_2 is the time constant associated with the magnetization decay in the transverse (x or y) directions. When the magnetic moments are rotated into the $x-y$ plane, they are initially in phase and have a net magnetic moment. However, due to spin-spin coupling, they eventually fall out of phase and thus produce no net magnetic moment. The rate of decay of the net magnetic moment in either the x or y directions is given in terms of T_2 as,

$$\frac{dM_{x,y}}{dt} = \gamma(\vec{M}\times\vec{B})_{x,y} - \frac{M_{x,y}}{T_2} \tag{9}$$

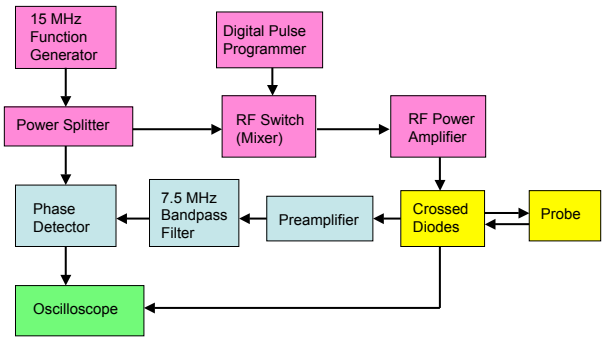

FIG. 3: Block digram of experimental setup. Components that provide the RF bursts to the sample are shown in pink, signal detection components are shown in blue.

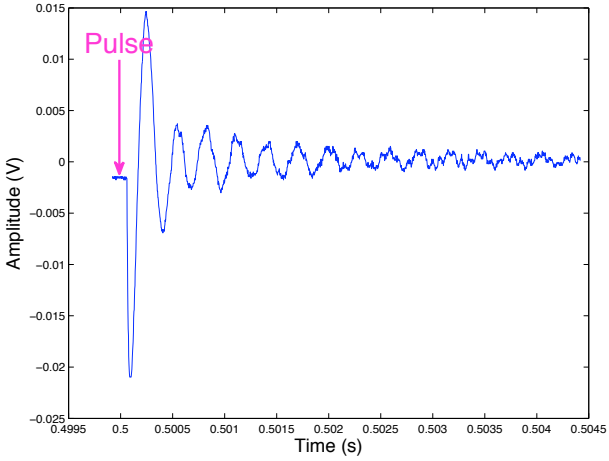

FIG. 4: Sample signal from a free induction decay. Approximate time of the pulse is indicated.

3. EXPERIMENT

3.1. General Setup

A large solenoid creates the large magnetic field B_0, and a small solenoid two centimeters long, wound with 10 turns of copper wire creates the weak oscillating field with frequency ω. We apply the weak oscillating field in short radio frequency (RF) pulses that rotate the ensemble average of the magnetic moment by a specified amount. This method is adventageous, because it allows us to separate the detection phase from the RF burst phase and use the solenoid to perform both. This method is essentially the same method that Bloch describes in his 1946 paper.[5] Figure 3 shows how we do this in practice. First, in the RF burst phase, the solenoid rotates the magnetic moment so that it has some component in the $x-y$ plane, where the large constant magnetic field B_0 causes it to precess at the Larmor frequency $\omega_0 = \gamma B_0$. Then, in the detection phase, the precessing magnetic field creates an alternating magnetic flux inside the solenoid, which by Faraday's law of induction induces an RF voltage in the solenoid. ω_0 is too high for us to observe directly on the oscilliscope, so we mix the induced voltage signal with the function generator frequency ω which is very close, to produce a beat frequency $|\gamma B_0 - \omega|$.

For the RF pulse part of our setup, a 15 MHz function generator passes through a power splitter to an RF switch. The digital pulse programmer sends the RF switch TTL logic that controls when the switch lets the function generator signal through. This signal then goes to the RF power applifier. When some component of the magnetic moments of the sample are rotated into the $x-y$ plane, the changing magnetic field produces a signal that decays exponentially as the phases of all the rotating magnetic moments decohere and eventually produce no net effect. This signal is called a free induction decay and is shown in figure 4. If the magnetic moments are rotated exactly 180^o, they will not precess about the z axis and we expect to see no signal. Experimentally, due to magnetic field inhomogeneity and other imperfections, we cannot perfectly rotate the net magnetic moment 180^o, so we do see some signal after a 180^o rotation. To come as close as possible to a 180^o pulse, we tune both B_1 by changing the amplitude output by the function generator and Δt by programming the Digital Pulse Programmer to minimize the free induction decay. We use 1.250 V peak to peak for the amplitude of the function generator, 50 ms for the 180^o pulse width, and $50/2 = 25$ ms for the 90^o pulse width.

3.2. Nuclear Magnetic Moments of Hydrogen and Fluorine

We find the frequency range with clear beats (close to resonance) and then vary the frequency to the frequency in that range where the beats disappear. By finding the ω such that $\omega = \gamma B_0$ we can find the nuclear magnetic moment of our sample. We found the magnetic moments of both hydrogen and fluorine by finding the resonant frequencies of glycerine and hexafluorobenzene, as the signals from the magnetic moments of hydrogen and fluorine are dominant in those molecules. For each sample, we took 5 statistically independent measurements of these frequency values by detuning and retuning the frequency. Also, the large magnet that produced $\vec{B_0}$ had different magnetic field settings for hydrogen and fluorine. Using a gaussmeter that we calibrated beforehand, we took 5 statistically independent measurements of the magnetic field for both of the settings. From this information, we could calculate the nuclear magnetic moments.

3.3. Measurement of the Spin-Lattice Relaxation Time T_1

Recall that the spin-lattice relaxation time T_1 is the time constant for a spin distribution's return to its nor-

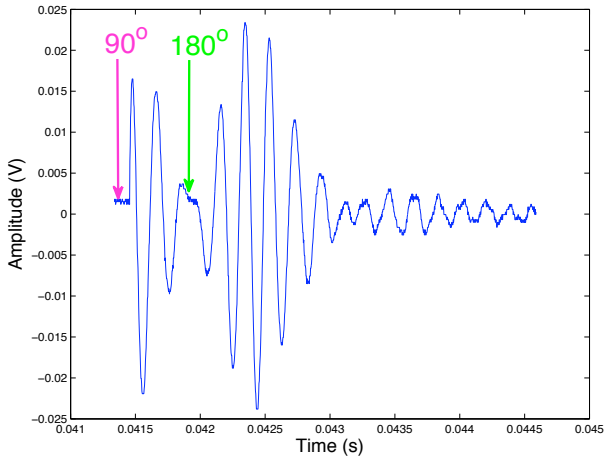

FIG. 5: Sample signal after the 90^o-T-180^o sequence in a 3 pulse sequence. Approximate times of the 90^o and 180^o pulses are indicated.

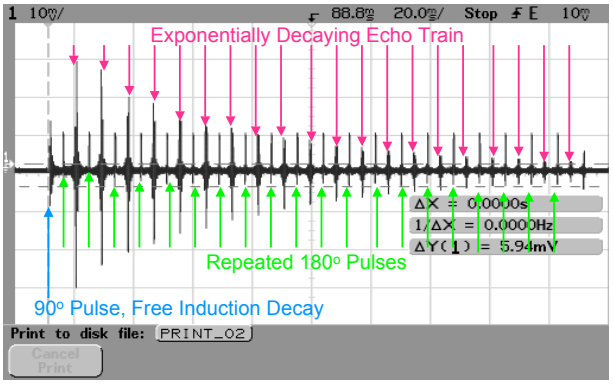

FIG. 6: Sample oscilloscope display for a Carr-Purcell pulse sequence. First a 90^o pulse is applied to rotate the magnetic moments into the $x-y$ plane. Then, repeated 180^o pulses are applied, which cause spin echoes that measure magnetization in the $x-y$ plane.

mal Boltzmann distribution after being perturbed. We determine T_1 by using a three pulse sequence. First we invert the population by applying a 180^o pulse that causes the spins to precess so that they point opposite $\vec{B_0}$. That is, we move the ensemble $\vec{\mu}$ average to point in the $-\hat{z}$ directon. Then we wait time τ and let some of the energy from the perturbation be coupled out to the sample's surroundings. Finally, we perform a 90^o-T-180^o sequence to determine how many of the spins have returned to the $|+z\rangle$ state. If a population of spins has returned to the $|+z\rangle$ state, the 90^o pulse will rotate the ensemble average into the $x-y$ plane, and we will see a free induction decay on the oscilloscope as the phases decohere. Then, after a short time T, the 180^o pulse rotates the spins from the $x-y$ plane, back to the $x-y$ plane and reverses all of the phases. T is kept small to minimize T_2 effects, which is one of the advantages of this particular sequence. This causes the phases to evolve backwards in time so that they recohere and decohere again, causing the oscilloscope signal to rise and then fall again. This phenomenon is called a spin echo. A sample oscilliscope trace from a three pulse sequence is shown in figure 5. In the three pulse sequence, the heights of the spin echoes are proportional to the number of spins that have returned to the $|z+\rangle$ state, so we measure these as a function of τ. We measured the pulse heights as a function of τ for 88%, 92%, 96% and 100% glycerine in aqueous solution, corresponding to viscosities of 150, 310, 644 and 1410 centiPoise/(mPa*s). Assuming that we were taking our measurements at 20^o C room temperature, we found the viscosities that corresponded to those concentrations from a chart given in the labguide[1]. No viscosity value was given for 88% concentration, so we extrapolated that value by looking at viscosity versus τ in that region. We also did the measurement for a paramagnetic ion in water solution of 10^{17} Fe^{+++} atoms/cc.

3.4. Measurement of the Spin-Spin Relaxation Time T_2: The Carr-Purcell Technique

Recall that T_2 is the time constant for magnetization decay in the $x-y$ plane. We determine T_2 by using the Carr-Purcell technique[6], which is a good technique especially for measuring longer T_2 times, as it minimizes diffision effects. We first rotate the magnetic field of the sample into the $x-y$ plane, then we wait time τ, and then apply a series of 180^o pulses, seperated by time 2τ. The 180^o pulses repeatedly time reverse the decoherence in the $x-y$ plane Between the series of 180^o pulses, we see spin echoes with height proportional to the magnetization in the $x-y$ plane. So, we expect the spin echo heights to decay exponentially with time constant T_2. A sample oscilloscope display for a Carr-Purcell pulse sequence is shown in figure 6. We perform the Carr-Purcell sequence for 88%, 92%, 96% and 100% glycerine in aqueous solution, corresponding to viscosities of 150, 310, 644 and 1410 centiPoise/(mPa*s). To find the amplitudes of the spin echoes, we take bitmap images of the oscilloscope display and use image editing software to map pixels to voltages.

From Slichter[4], we find the relationship between the magnetization and the number of 180^o pulses,

$$M(n2\tau) = M_0 e^{-\gamma \frac{\partial H}{\partial z}^2 D(n2\tau)\frac{1}{3}\tau^2} e^{\frac{-n2\tau}{T_2}} \qquad (10)$$

The first exponential is a second order effect, because the argument is proportinal to τ^2, so we ignore it and fit to the second exponential.

4. DATA AND ANALYSIS

4.1. Magnetic Moments

First, we solve for the magnetic moment μ in terms of our measured variables ω_0 and B_0,

$$\omega_0 = \gamma B_0 = \frac{\mu}{I\hbar} B_0 \Rightarrow \mu = \frac{\omega_0 I\hbar}{B_0} = \frac{\pi \nu_0 \hbar}{B_0} \qquad (11)$$

For hydrogen, we measured ν_0 to be 7.52203 ± 0.00002 Hz and B_0 to be 0.17676 ± 0.0006 Tesla. We calculated μ to be $(1.4099 \pm .0048) * 10^{-26}$ Joules/Tesla. This is approximately 3 standard deviations from $\mu = 1.4131 * 10^{-26}$ Joules/Tesla calculated from values given in the lab guide. We only found the statistical errors, and our values were statistically well-determined, so our errors were extremely small. Inhomogeneity in B_0 is a good candidate for systematic error. In the future, we should take measurements that determine how much we can expect B_0 to vary over the distance range our sample occupies.

For fluorine, we measured ν_0 to be 7.52224 ± 0.00005 Hz and B_0 to be 0.17676 ± 0.0006 Tesla. We calculated μ to be $(1.4094 \pm 0.0056) * 10^{-26}$ Joules/Tesla. The presently accepted value of μ, obtained from webelements.com[7], is $1.3278 * 10^{-26}$ Joules/Tesla. Given our ν_0 uncertainty for fluorine, our μ value is very far away from the accepted value. Also, our μ value is suspiciously close to the μ we calculated for hydrogen. Perhaps some of the test tubes in the sample rack were switched and we were looking at the wrong sample. This is another question to investigate.

4.2. Spin-Lattice Relaxation Time T_1

We measured the spin echo height in the three pulse sequence as a function of τ. We did the three pulse sequence slightly off resonance, so we saw several oscillations in the spin echo, as shown in figure 5. To find the spin echo height, we found the height of the oscillation with the highest amplitude within the envelope. The raw data was exported from the oscilloscope directly to the computer. To find the statistical error on the spin echo height, we saved the oscilloscope output for 88% glycerine 5 different times and found the standard deviation of the heights to be 11.15%. The 5 different amplitudes near the peak as a function of data point number are shown in figure 7. We assumed that the other amplitudes that we measured would also have 11.15% error. To reduce error, we could better determine the pulse amplitude by measuring the oscilliscope output 5 different times for every τ value and sample.

For each of the samples, we fit our amplitude versus τ data to the function $A(1 - e^{-\tau/T_1})$ and found T_1. The fit for 310 cP/(mPa*s) glycerine is shown in figure 8. For all of our amplitude versus τ plots, the shape of our theoretical function clearly does not match the shape of our data. This is particularly evident in our residuals, as they have very clear structure.

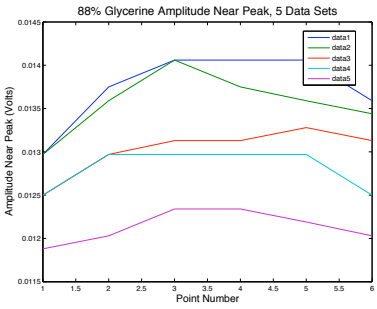

FIG. 7: 5 different measurements of amplitude near the peak of the three pulse sequence spin echo, for 88% glycerine.

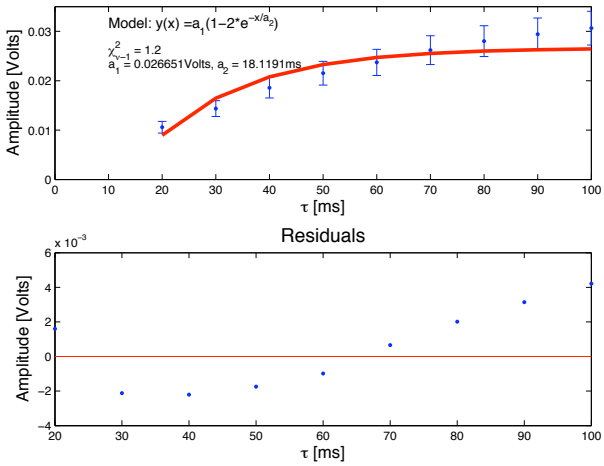

FIG. 8: Exponential fit to determine T_1 in 310 cP/mPas glycerine, a 92% aqueous solution. The fit does not follow the shape of the data, and the residuals have a very clear structure, indicating that the data does not follow the theoretially predicted function.

The T_1 values that we measured for the different viscosities are listed in table I. Our results do not agree with Bloembergen's[8] results. Bloembergen shows a negative linear relationship on a log-log plot of T_1 versus viscosity and over the viscosity range we are considering, Bloembergen finds that T_1 varies by an order of magnitude, whereas our T_1 values do not very much at all. We also expect our T_1 values to monotonically decrease as a function of viscosity, but that is not the case.

Viscosity (Cp/mPas)	T_1 (ms)
150	20.2945 ± 1.0425
310	18.1191 ± 1.1684
624	19.0877 ± 0.5998
1410	8.9033 ± 0.5979

TABLE I: T_1 values measured for different viscosities of glycerine. These results do not agree with Bloembergen[8].

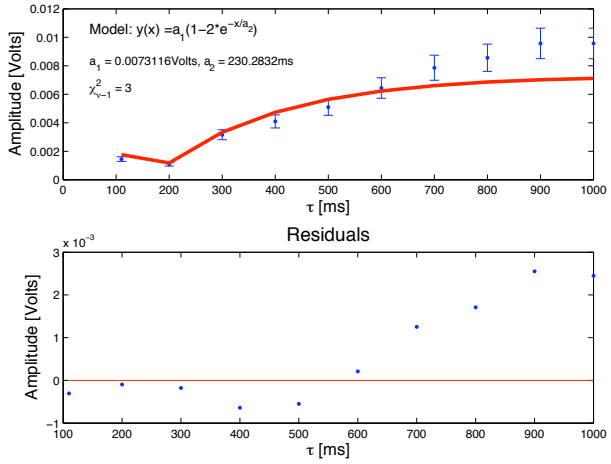

FIG. 9: Exponential fit to determine T_1 in 10^{17} Fe^{+++}/cc solution. As for the exponential fit for glycerine, the fit does not follow the shape of the data, and the residuals have a very clear structure, indicating that the data does not follow the theoretically predicted function.

For 10^{17} Fe^{+++} ions/cc, the exponential fit for amplitude versus τ, shown in figure 9, was also poor, as the fit did not follow the shape of the data and the residuals had clear structure. In the future, we wish to find the T_1 values for different paramagnetic ion concentrations so we can establish a relationship.

4.3. Spin-Spin Relaxation Time T_2

We used to the Carr-Purcell sequence to determine the spin-spin relaxation time T_2. We found the echo heights by taking a bitmap image screen shot of the oscilloscope trace and looking at it in image editing software. For the error in echo amplitudes, we added in quadrature the statistical variation found earlier the error in pixel determination and the error in oscilloscope resolution. To find T_2 we fit exponential functions Ae^{-t/T_2} to our data. Figure 10 shows the fit for 310 cP/(Pa*s) glycerine. Our fits to determine T_2 followed the data and had reduced chi-squared values close to 1. The errors on T_2 were determined by the fitting algorithm.

We plotted T_2 as a function of viscosity and found a negative linear relationship on a log-log plot, in agreement with Bloembergen[8]. We used error propogation methods to find our errors on the log-log plot, given our errors on T_2. Qualitatively, it makes sense that T_2 should decrease as a function of viscosity, because the molecules in more viscous fluids are more strongly coupled to each other.

Given time constraints, we were not able to find exponentially decreasing echos for different concentrations of paramagnetic ions.

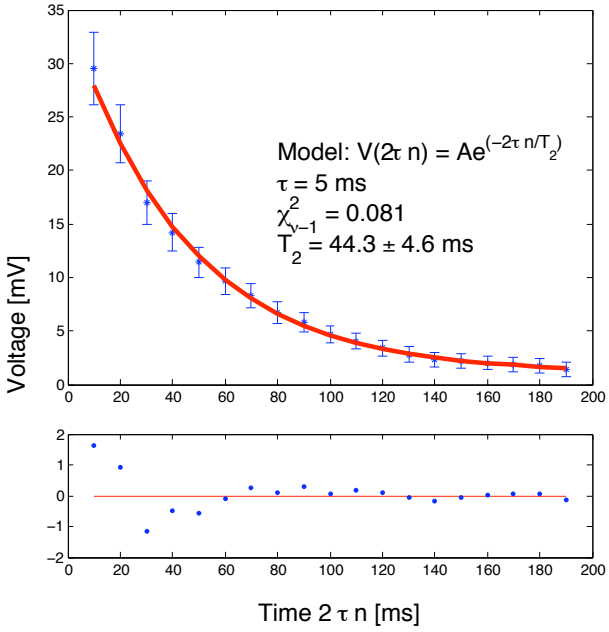

FIG. 10: Exponential fit to determine the spin-spin relaxation time of 310 cP/(Pa*s) glycerine, a 92% aqueous solution. The fit follows the shape of the data and our reduced chi-squared value is close to 1, indicating reasonable errors.

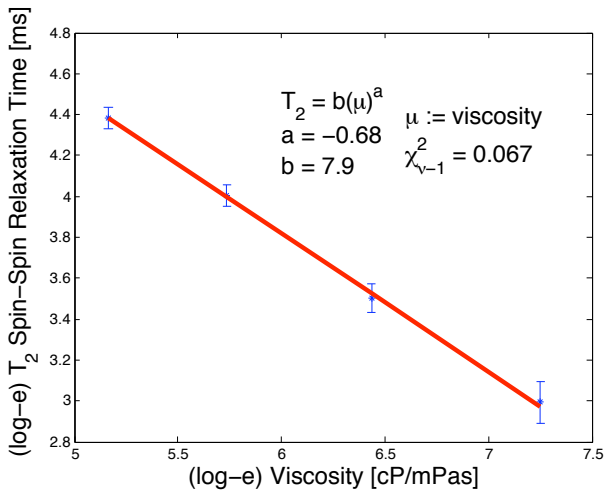

FIG. 11: Spin-spin relaxation time T_2 as a function of viscosity.

5. SOURCES OF LARGE ERROR IN T_1 DETERMINATION

Our values for T_1 are far from the values in the literature, they do not follow the trend as a function of viscosity that we would expect, and the exponential fits that determined them were poor. The errors that we calculated do not explain these differences. We now suggest errors in experimental procedure and analysis technique that could have produced these discrepancies. One possibility is that our pulse widths were not tuned correctly.

For our 180^o pulse settings, when we varied B_1 and Δt in either direction, we saw the amplitude of the free induction decay increase, so we were reasonably confident that we picked the right amplitude and time. However, we could be more sure if we actually plotted the 180^o free induction decay amplitude as a function of time and as a function of amplitude and verified that we were operating at the minimum. Another problem was our fit algorithm that was supposed to fit our data to the function $A(1 - e^{-t/T_1})$. We used the "levmar" Matlab file from the Junior Lab website, which is an implementation of the Levenberg-Marquardt algorithm. This algorithm takes some initial values for the A and T_1 parameters and searches for the local chi-squared minimum. When doing the fits, we there appeared to be many closely-spaced local minima. Small variations in the initial parameters would give us completely different values for T_1. We suspect that this effect occured because our data itself was bad and did not follow the shape of the theoretical function. Therefore, none of the fits were particularly good. However, it is definitely still something to investigate further. Perhaps in the future we can try using a more robust algorithm. Finally, the most likely reason for our poor T_1 results was that the three pulse sequence requires us to operate almost directly on resonance. We made the mistake of moving our function generator off resonance because we thought we could get a better value for the amplitude of the echo if we were looking at a wide envelope of oscillations. However, the wide envelope of oscillations for both the free induction decay after the 90^o pulse and the spin echo after the 180^o pulse makes observations confusing because the free induction decay and the echo can sometimes overlap.

6. CONCLUSIONS

In this experiment, we measured the nuclear magnetic moment of hydrogen to be $(1.4099 \pm .0048) * 10^{-26}$ Joules/Tesla and the nuclear magnetic moment of fluorine to be $(1.4094 \pm 0.0056) * 10^{-26}$ Joules/Tesla. We attempted to measure the spin-lattice relaxation time T_1 using the three pulse sequence, but our data was poor, probably because our frequency generator was set somewhat off resonance. We succesfully measured the spin-spin relaxation time T_2 by using the Carr-Purcell pulse sequence, and found a negative linear relationship on a log-log plot of T_2 versus viscosity for different viscosities of glycerine. In all cases, we see qualitatively the expected free induction decay and spin echo behavior.

Later this term we will have an opportunity to: double check our magnetic moment measurements, refine our pulse width tuning, take more statistically independent measurements of echo heights to better constrain our values and determine statistical error, experiment with different fitting algorithms, try the three pulse sequence closer to resonance, and get T_1 and T_2 data for both different viscosities of glycerine and for different paramagnetic ion concentrations in water.

[1] S. Sewell, *Pulsed Nuclear Magnetic Resonance: Spin Echoes* (2008).
[2] J. Negele, *8.05 course notes* (2008).
[3] R. Baierlein, *Thermal Physics* (Cambridge University Press, New York City, 1999).
[4] C. P. Slichter, *Principles of Magnetic Resonance* (Springer-Verlag, New York, 1990), 3rd ed.
[5] F. Bloch, Physical Review **70**, 460 (1946).
[6] H. Y. Carr and E. M. Purcell, Physical Review **94** (1954).
[7] *Nmr properties of fluorine*, URL http://www.webelements.com/fluorine/nmr.html.
[8] N. Bloembergen, E. M. Purcell, and R. V. Pound, Physical Review **73** (1948).

Acknowledgments

S. Campbell acknowledges Javier D.'s equal contribution to this experiment and analysis. S. Campbell also thanks Daniel Furse, Natania Antler, Professor David Litster, Regina Yopak and Emily Edwards for their advice and hard work on this course.

Pulsed Nuclear Magnetic Resonance

Joan C. Smith*
MIT Department of Physics
(Dated: February 25, 2011)

In this experiment the phenomena of nuclear magnetic resonance is used to determine the magnetic moments of the proton and fluorine nucleus. The magnetic moment of the proton is found to be $\mu = (1.41 \pm 0.14) \times 10^{-23}$erg/gauss and the magnetic moment of the fluorine nucleus is found to be $\mu = (1.33 \pm 0.13) \times 10^{-23}$erg/gauss. To measure the magnetic moments, radio frequency pulses are applied to a sample in a large homogenous magnetic field. By tuning the applied frequency to the resonance frequency of the sample, the magnetic moments can be calculated. Measurements are performed to relate the spin-spin and spin-lattice relaxation times of glycerin to viscosity. Using the same apparatus, the spin-spin and spin-lattice relaxation times are measured by applying sequences of rf pulses to the samples. The relationship found between the viscosity of glycerin samples and their relaxation times is within 2σ of the accepted value from literature.

1. INTRODUCTION

Individual particle spins are related to single particle magnetic moments by a constant factor. Nuclear magnetic resonance is a technique to measure the magnetic moment of nuclei in a sample. Nuclei are made up of protons and neutrons, each of which are spin $\frac{1}{2}$ particles. For a particle with total spin $\frac{1}{2}$, spin in the $+z$ direction can be either $+\frac{1}{2}$ or $-\frac{1}{2}$.

In nuclear magnetic resonance experiments a classical approximation is used to understand the behavior of particle spins.

2. NUCLEAR MAGNETIC RESONANCE AND RELAXATION TIMES

2.1. Theory of NMR and Classical Approximation

By considering an ensemble of spins in a sample we can use the classical understanding of angular momentum to approximate the behavior of many spins.

Each ensemble can be thought of as a total magnetic moment of many spins. In an ensemble there can be spins pointing in any direction, the resulting total magnetic moment vector can have components in any direction. By considering this ensemble of spins, the classical understanding of angular momentum can be used.

The total magnetic moment of an ensemble of spins is $\vec{\mu} = \gamma \vec{I}$, where γ is the gyromagnetic ratio for the relevant nucleus and $\vec{I}$ is the total angular momentum of the ensemble. In the classical approximation, placing a particle with magnetic moment $\vec{\mu}$ in a magnetic field $\vec{B}$ produces a torque τ, causing the magnetic moment to precess about the direction of the applied magnetic field.

$$\tau = \vec{\mu} \times \vec{B_0} \tag{1}$$

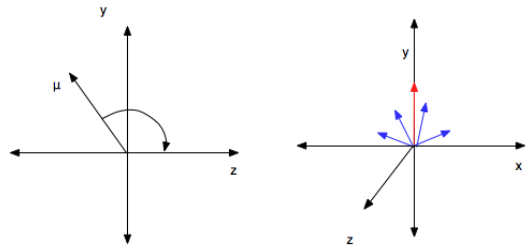

(a)Spin-Lattice Relaxation Time (b)Spin-Spin Relaxation Time

FIG. 1: Illustration of effect of Spin-Lattice and Spin-Spin relaxation times.

Since torque is $\frac{d\vec{I}}{dt}$, the Larmor frequency ω_0 can be computed to be

$$\vec{\omega_0} = -\gamma \vec{B_0} = -\frac{g\mu_n \vec{B_0}}{\hbar} \tag{2}$$

$\vec{\omega_0}$ is called the Larmor Frequency and is the resonance frequency of the ensemble of spins in a magnetic field. Finding the Larmor frequency allows the calculation of μ, the magnetic moment of the nucleus. This resonance phenomena also allows the measurement of the spin-lattice relaxation time and the spin-spin relaxation time, called T_1 and T_2 respectively. [1]

2.2. Relaxation Times

Nuclear magnetic resonance involves a sample placed large constant magnetic field in the $+\hat{z}$ direction, and a small oscillating magnetic field applied primarily in the $\hat{x}$ direction. Subsequently, the oscillating field is turned off, and the magnetic moments decay back to a thermal state. The spin-spin and spin-lattice relaxation times are measures of how the magnetic moments decay back into the the xz plane.

The spin-lattice relaxation time is a measure of the time it takes for spins to decay back to alignment with the

*Electronic address: joans@mit.edu

large magnetic field after they have been excited. A large magnetic field in the $+\hat{z}$ direction causes states where the spins are aligned with the field to have a lower energy configuration. As energy dissipates from the protons due to electromagnetic interaction, more spins will become aligned along the large magnetic field, as shown in Fig. 1(a).

The spin-lattice relaxation time, called T_1 is the time constant for this exponential decay.

The decay involved in spin-spin relaxation time does not change the energy of the system. It is local and quantum mechanical; the effect is between protons in nuclei that are slightly out of alignment in the direction transverse to the large magnetic field. The spin-spin interaction of these unaligned particles causes increasing transverse decoherence.

2.3. Relaxation Times and Viscosity

The relationship between viscosity and relaxation times is measured. In viscous materials, to a zeroth order approximation the molecules are closer together than they are in a less viscous material. Both spin-spin and spin lattice relaxation times are determined by the coupling of magnetic fields in protons to magnetic fields in the surrounding environment. Since molecules are closer together in viscous samples, the interactions will be stronger, the stronger interactions will return the sample to equilibrium faster. The spin-spin relaxation time and the spin-lattice relaxation time will decrease as the viscosity increases.

3. EXPERIMENTAL SETUP

The necessary small magnetic field is applied by generating radio frequency pulses that produce a magnetic field. The rf pulses are applied for different durations. The pulse durations correspond to rotating the spins in the sample by a specified angle. Combinations of pulses of different frequency and duration are used to probe characteristics of the sample.

3.1. Experimental Apparatus

This experimental apparatus has five main components: two large permanent magnets, a radio frequency pulse generator, a probe circuit that the sample sits in, and a phase detector that mixes the input signal from the frequency generator and the output Larmor frequency signal from the sample together. An oscilloscope is used to view and collect data.

The permanent magnets are used to produce the large magnetic field, measured to be $(1.768 \pm 0.180) \times 10^3 G$. The error on this measurement takes into account 10% inhomogeneity in the magnetic field. A sample, glycerin, water or flourine, is placed in the probe circuit between the two large magnets. The sample sits in a solenoid that measures the magnitude of the magnetization in the $+z$ direction.

A set of tunable capacitors in the probe circuit are used to ensure a visible signal. The probe circuit is placed under the sample, and connected to the pulse generator and filtering electronics by way of input and output cables. The output signal from the proton spins is mixed with the output signal from the pulse generator. The result is beating between the two signals that is visible on the oscilloscope.

4. DATA AND ANALYSIS

4.1. Method for Measuring Magnetic Moments

To calculate the magnetic moment of a sample, the Larmor frequency of that sample is measured. The Larmor frequency is related to the magnetic moment by equation 2 and $\vec{\mu} = \gamma \vec{I}$. When a magnetic field is applied, the spins in the sample will precess with the said frequency. When the input frequency on the pulse generator is the Larmor frequency, the beating terms vanish.

A sample of glycerin, $C_3H_5(OH)_3$, is placed in the solenoid to measure the magnetic moment of the proton in hydrogen. Once the adjustable capacitors are tuned to see a signal, a series of pulses are applied in order to determine the correct duration for a pulse that rotates the spins in the sample by 180°.

The frequency on the frequency generator is tuned such that there is a large free induction decay (FID) viewed on the oscilloscope. The FID is an exponentially damped sinusoid, due to the mixing of the NMR output signal with the frequency input signal, as described above. The time constant on the exponential damping is T_1, the Spin-Lattice relaxation time. The measurement of T_1 will be discussed in detail in Sec. 4.2. To calculate the magnetic moment of the proton, a so-called 90° pulse is applied. A 90° pulse is a pulse of duration t that rotates the spins in the sample 90° around the z-axis, into the xy plane.

In order to determine t, we sweep through pulse durations, from $1\mu s$ to $100\mu s$. The 180° pulse produces no FID, or a minimal amplitude FID. Under these conditions, the spins of the protons will have no components parallel to the solenoid. Since there is no parallel component, there will be no emf induced in the solenoid, and thus no signal. Once the 180° pulse is found, its duration is halved to find a 90° pulse.

Once a 90° pulse is found, a series of repeating 90° pulses are applied to the sample, producing FIDs. The frequency generator is tuned between each 90° pulse. As the frequency approaches the Larmor frequency, the effect of beating between the mixed input and NMR output signals approaches the resonance condition. The frequency at resonance is recorded to calculate the magnetic moment using Eq. 2.

4.2. Method for Measuring T_1

T_1, the spin-lattice relaxation time is measured using two different methods. The first method is to apply a series of 2-pulse sequences. The first pulse in the sequence has the duration determined previously to produce a 90° rotation. A time τ allows the spin-lattice relaxation to occur, and is followed by a second 90° pulse.

The first pulse moves the spins into the xy plane. The time τ allows the spins to decay back toward the z-axis. Once the pulses have decayed, the second 90° pulse is applied. This second pulse rotates the spins 90° about the $z - axis$, such that the net magnetization vector is positioned as in Fig 1(a). The spins are then allowed to decay again, back to alignment in the z-axis.

Data is collected following the second pulse. This signal is an FID whose magnitude is proportional to the magnitude of the magnetic moment vector that has decayed completely into alignment with the z-axis. As tau is varied, the amplitude of the FID should decrease, since when more time elapses between the first pulse and the second, more magnetization has decayed completely into the $\hat{z}$ direction. The result of this sequence will be a descending decaying exponential, whose time constant is T_1. This pulse sequence is therefore useful for measuring T_1 for samples where T_1 is expected to be short.

The second method used to measure T_1 employs a 180° pulse, followed by a delay τ, and a 90° pulse. This pulse sequence rotates the spins first 180° producing no FID. The delay τ allows the spins to decay toward the z axis. The 90° pulse rotates spins back toward the xy plane. As in the previous pulse sequence, T_1 is measured by varying τ, and measuring the amplitude of the FID produced after the last pulse. In this method, the amplitude of the FID will be maximal when τ is larger than T_1. In time τ, the magnetization is entirely aligned with the magnetic field, causing the 90° pulse to rotate the spins back to the xy plane. Once τ is sufficiently large the magnitude of the FID stabilizes.

This method lends itself to measuring long T_1s, as spins must decay further, from 180° to 0°, rather than from 90° to 0°.

4.3. Method for Measuring T_2

T_2, the time constant for spin-spin relaxation is measured with one of two methods. The first method is a simple pulse sequence, similar in nature to those used to measure T_1. This pulse sequence is a 90° pulse, followed by a delay τ, followed by a 180° pulse.

A spin-echo occurs a time τ after the 180° pulse in this sequence. The 90° pulse rotates the spins from the $\hat{z}$ axis up to the $\hat{x}$ direction. A time τ passes, letting the spins decay transversely, spreading out in the xy plane. The 180° pulse inverts the spins, but they continue moving in the same direction. The result is that the spins recohere, producing a signal again. As the spins decohere the signal

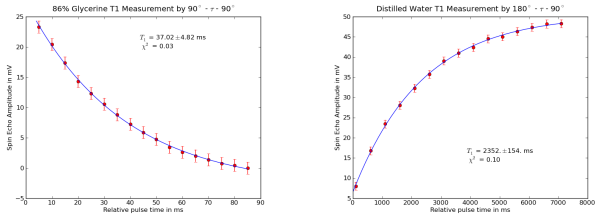

(a)T_1 Measurement with 90° -τ 90° pulse sequence (b)T_1 Measurement with 180° -τ 90° pulse sequence

FIG. 2: Data collected by the two methods for measuring T_1

induced in the solenoid becomes smaller, since there is less magnetization in the $\hat{z}$ direction. After the 180°, the spins rotate back through the xy plane while recohering. The result is a signal that begins rising τ after the 180° pulse, reaches a maximum and falls again. This rising and falling signal is the spin-echo.[2]

By varying τ and measuring the amplitude of the spin-echo produced, a decaying exponential is plotted. The exponential's decay constant is T_2[3].

The second method for measuring T_2 is the Carr-Purcell sequence. The Carr-Purcell sequence also begins with a 90°-τ-180° pulse sequence. Instead of repeating this pulse sequence manually, varying τ, the Carr-Purcell sequence uses a delay of 2τ, then another 180° pulse, then another delay of 2°, and so on. Each 2τ-180° pulse sequence allows the spins to further decohere in the transverse plane. The result is a decaying exponential that can be fit to produce values for T_2.

4.4. Determining Magnetic Moments

The method for determining the magnetic moment of the proton was described above. By tuning the frequency generator, resonance was found to be $\omega_0 = 7.52196 \times 10^6 \frac{rad}{s}$. Converting this to a frequency and using $\mu = \frac{\omega_0 \hbar}{2B_0}$, $\mu = (1.41 \pm 0.14) \times 10^{-23} \frac{ergs}{gauss}$. For the flourine nucleus, $\omega_0 = 7.0760 \times 10^6 \frac{rad}{s}$, giving $\mu = (1.33 \pm 0.13) \times 10^{-23} \frac{ergs}{gauss}$[4]. Each of these values differ by less than one standard deviation from the accepted values[5].

4.5. Determining T_1 and T_2

T_1 and T_2 were measured for different concentrations of glycerine, ranging from 100% glycerine to distilled water. T_1 and T_2 were measured using the methods above, and fit to the appropriate exponentials. Sample data is shown in Figs. 2(a) and 3. Descending exponentials were fit to $f(x) = Ae^{-\tau/T} + B$. Rising exponentials, like those produced by the 180° - τ - 90° pulse sequence used to measure T_1 as in 2(b) were fit to $f(x) = A(1 - 2e^{-\frac{\tau}{T}}) + B$. The data are shown in Table I. The error bars on

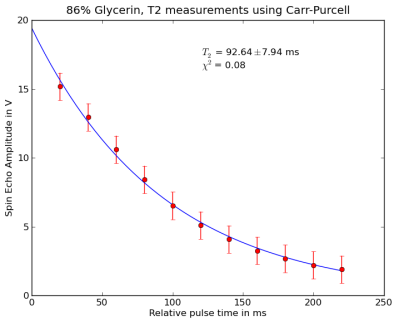

FIG. 3: Sample data collected for measurement of T_2 for 86% Glycerine sample. Data was collected using the Carr-Purcell method for spin-echo measurement.

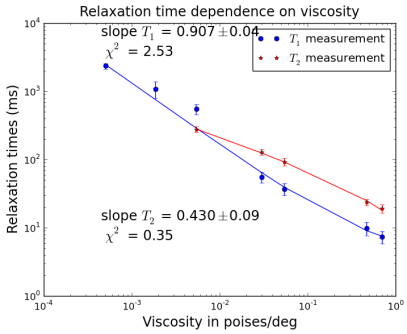

FIG. 4: Results plotted on a log-log scale for different viscosities of glycerine. Blue data points are measurements of T_1, and red data points are measurements of T_2.

both the T_1 and T_2 measurements were calculated by adding in quadrature the standard deviation of each of the three trials for each data point and the uncertainty in the amplitude measurement from the oscilloscope. This uncertainty was .3 mV.

4.6. Relationship between Relaxation Time and Viscosity

By measuring relaxation times for samples of varying viscosity, we establish that within the range measured both T_1 and T_2 decrease as the viscosity of the sample increases.

This plot has Pa per degree on the x axis. In order to probe further range of viscosities, we intended to cool the different concentration glycerine samples. By normalizing this graph by temperature, these samples would be comparable at different temperatures. Due to time constraints we were unable to perform this procedure. By fitting the log of the data for T_1 and T_2 to linear functions, the slope of the power laws were obtained. Error on each data point was taken to be the error produced by the T_1 and T_2 fit functions. The relationship was fit to a power law, as expected. The slope of the T_1 fit was found to be -0.91 ± 0.04, the slope of the T_2 fit was found to be 0.43 ± 0.10. This varies from the Bloembergen and Purcell of -1 measurement by 2σ in the case of T_1. The measurement for T_2 is significantly less accurate because data were unable to be obtained for very low concentrations of glycerine.[6].

Percent Glycerine	T_1 (ms)	T_2 (ms)
Distilled Water	2352.98 ± 154.12	-
40	1087.08 ± 199.90	-
60	549.42 ± 62.43	275.72 ± 17.85
80	55.57 ± 6.70	128.84 ± 8.54
86	37.03 ± 4.82	92.64 ± 7.94
98	9.84 ± 1.44	23.55 ± 1.71
100	7.31 ± 1.02	19.18 ± 1.74

TABLE I: T_1 and T_2 collected for different concentrations of glycerine

5. CONCLUSIONS

In conclusion, the values calculated for the magnetic moment of the proton and flourine nucleus were $\mu = (1.41 \pm 0.14) \times 10^{-23}$erg/gauss and $\mu = (1.33 \pm 0.13) \times 10^{-23}$erg/gauss, respectively. These values are both within σ of the accepted values.

The viscosity relaxation time relationship was found to agree well with the relationship presented by Bloembergen in the 1954 paper[6]. The value for the relationship between T_1 and viscosity was within 2σ of that measured by Bloembergen. The T_2 measurements were less in agreement because fewer measurements were performed.

In order to confirm the behavior of high viscosity T_1 and T_2 relationships, in further experiment the different concentrations of glycerine will be cooled in order to change the viscosity of the samples.

[1] A. Melissinos, *Techniques in Experimental Physics* (Academic Press, 2003), chap. Magnetic Resonance Experiments.
[2] E. Hahn, *Spin echos* (1950).
[3] H. Carr and E. Purcell, Phys. Rev. (1954).
[4] P. Bevington and D. Robinson, *Data Reduction and Error Analysis for the Physical Sciences* (McGraw-Hill, 2003).
[5] D. R. Lide, ed., *CRC Handbook of Chemistry and Physics* (2010), 91st ed.
[6] E. P. N. Bloembergen and R. Pound, Phys. Rev. (1948).

Nuclear Magnetic Resonance and the Measurement of Spin-Spin Relaxation Times

Javier M. G. Duarte* and Sara L. Campbell†
Massachusetts Institute of Technology, MA 02142
(Dated: November 4, 2008)

We use the experimental technique of pulsed nuclear magnetic resonance (NMR) to measure magnetic and spin relaxation properties of several different solutions. We measure the magnetic moments of hydrogen and fluorine to be $\mu_H = (1.4099 \pm .0048) \times 10^{-26}$ Joules/Tesla and $\mu_F = (1.4094 \pm .0056) \times 10^{-26}$ Joules/Tesla, respectively. The effect of viscosity on spin-lattice relaxation time, T_1, and spin-spin relaxation time, T_2, is determined by testing various aqueous glycerine solutions. Data was also taken for solutions with varying paramagnetic ion (Fe^{+++}) concentrations, however low statistics, among other factors, limited the analysis. For spin-spin relaxation, the negative linear relationship is confirmed between the natural logarithms of viscosity and T_2.

I. INTRODUCTION

The natural phenomenon of magnetic resonance arises in systems due to the interplay of magnetic moments and angular momentum. Though the magnetic resonance of atoms was known and studied by many, including I. I. Rabi and collaborators in 1939, the nucleus was not probed until late 1945. Nearly simultaneously, F. Bloch and E. M. Purcell independently discovered nuclear magnetic resonance (NMR), in which a magnetic field breaks the energy degeneracy of different spin states and transitions between these states may be observed [1].

E. Hahn later made the discovery of "spin echoes" using pulsed NMR techniques, which led to the invention of a plethora of pulse sequences to measure magnetic properties of atoms. Two of these properties are the spin-lattice relaxation time T_1, a measure of how long it takes an ensemble of spins to reestablish the Boltzmann equilibrium, and spin-spin relaxation time T_2, the characteristic time for the transverse magnetization to decay.

In this experiment, we study each sample placed in the field of a permanent magnet by applying pulses of a transverse RF magnetic field and interpreting the effects on the overall magnetization.

II. THEORY

We follow the general discussion outlined by [1] with additional material from [2].

A. Larmor Spin Precession

A spin 1/2 particle with magnetic moment $\vec{\mu} = \gamma \vec{S}$ in a static magnetic field, $\vec{B} = B_0 \vec{n_z}$ solely in the z-direction, has a Hamiltonian,

$$\hat{H} = -\vec{\mu} \cdot \vec{B} = -\gamma B_0 \hat{S}_z, \tag{1}$$

where $\hat{S}_z$ is the z-direction spin operator and $\gamma = g\mu_N/\hbar$ is specific to the

Then, we can define the vector $\vec{J} = (\langle \hat{S}_x \rangle, \langle \hat{S}_y \rangle, \langle \hat{S}_z \rangle)$ of the expectation values of the spin operators, which behaves like the classical angular momentum vector. Particularly, we know that torque is related to angular momentum by,

$$\vec{\tau} = \vec{\mu} \times \vec{B} = \gamma(\vec{J} \times \vec{B}) = \frac{d\vec{J}}{dt}. \tag{2}$$

Classical gyroscopic precession yields the solution of equation 2,

$$\vec{\omega_0} = -\left| \frac{d\vec{J}/dt}{\vec{J} \times \vec{n}_z} \right| \Rightarrow \omega_0 = \gamma B_0. \tag{3}$$

This quantity is called the Larmor frequency and it is the rate at which the classical vector J precesses about the constant magnetic field; see figure 1 for an illustration.

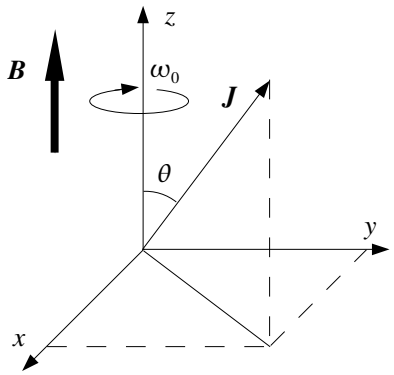

FIG. 1: Larmor precession of the classical spin vector J about the constant magnetic field B. Modified from [1]

The preceding discussion is sometimes referred to as the classical description of NMR. We may also view the quantum picture of the same phenomenon in a slightly different situation.

*Electronic address: woodson@mit.edu
†Electronic address: campsoup@mit.edu

B. Nuclear Magnetic Resonance

If we apply static and time-dependent circularly-polarized orthogonal magnetic fields,

$$\vec{B}(t) = (B_1 \cos\omega t, -B_1 \sin\omega t, B_0), \tag{4}$$

we see that the Hamiltonian does not commute with itself at different times: $[\hat{H}(t_1), \hat{H}(t_2)] \neq 0$ for some $t_1 \neq t_2$ [2]. One implication of this is that we cannot use the unitary time evolution operator $\hat{U} = e^{-i\hat{H}t/\hbar}$ to find the form of a state at later times. However, we can employ a basis transformation into the frame rotating about the z-axis with angular frequency ω, the driving frequency of the applied magnetic field.

First, we begin with the Hamiltonian in the lab frame and manipulate it,

$$\begin{aligned} \hat{H} &= -\gamma B_0 \hat{S}_z - \gamma B_1 (\hat{S}_x \cos\omega t - \hat{S}_y \sin_{\omega t}) \\ &= e^{i\omega t \hat{S}_z/\hbar}(-\gamma B_0 \hat{S}_z - \gamma B_1 \hat{S}_x) e^{-i\omega t \hat{S}_z/\hbar}, \end{aligned} \tag{5}$$

so that we achieve the form $\hat{H} = \hat{\mathcal{U}}^\dagger \hat{H}_{\rm R} \hat{\mathcal{U}}$, where $\hat{\mathcal{U}}$ is a change of basis unitary transformation and $\hat{H}_{\rm R}$ is the Hamiltonian in the new, rotating frame. Its form dictates that this frame of reference has an effective magnetic field,

$$\vec{B}_{\rm eff} = (B_0 - \frac{\omega}{\gamma})\vec{n}_z + B_1 \vec{n}_x, \tag{6}$$

which gives rise to the resonance condition of $\omega = \omega_0 = \gamma B_0$, the Larmor frequency.

NMR techniques, including the use of pulsed radio frequency (RF) signals, have been used to make a wide variety of measurements, one of the most prevalent is that of the spin relaxation times, T_1 and T_2.

C. Spin-Lattice and Spin-Spin Interactions

Several factors contribute to the behavior of the magnetization of a large ensemble of spins when the magnetic field of equation 4 is present, including spin-lattice interactions, spin-spin interactions, and magnetic field inhomogeneity.

The fact that the magnet is not completely uniform causes individual particles in different locations to precess at slightly different frequencies so they gradually decohere, that is get out of phase with one another.

The spin-lattice relaxation time T_1 is associated with the approach to thermal equilibrium. In other words, it is the characteristic decay time for the return to the Boltzmann distribution. It is also a measure of how quickly the longitudinal magnetization returns to equilibrium.

On the other hand, the spin-spin relaxation time T_2 is associated with the transverse magnetization rate of decay. It is a measure of how fast the spins recohere and decohere in the transverse plane. Since T_1 is related to the "cooling" of the sample, whereas T_2 is only related to the coupling of spins between magnetized particles, T_1 must be greater than T_2; A particle which has been returned to equilibrium with the static magnetic field (in the z-direction) cannot contribute to the transverse magnetization.

III. EXPERIMENTAL DESIGN

A. Setup

First, we take a sample in a small test tube and suspend it between two strong magnets inside of a solenoid.

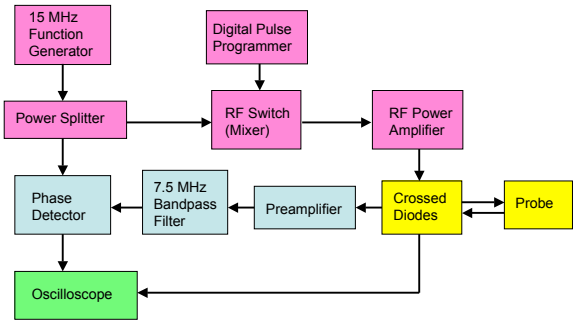

FIG. 2: Block diagram of the experimental setup created by S. Campbell.

We introduce an RF sinusoid waveform from a pulse generator into the signal chain, which is split, with half of it directed to one of the inputs (the reference) of the phase detector and the other half sent through an RF switch, which is controlled by the digital pulse programmer (DPP). The DPP allows the experimenter to manipulate the number of, delay between, and time duration of pulses. After the switch, the pulse is amplified and sent to the sample, which is a part of the probe circuit.

The probe circuit is composed of two tunable capacitors, one in series with the sample adjusted for impedance matching, while the other is in parallel with the combination of the capacitor and sample and it is tuned to the frequency of the input RF signal. The RF pulse enters the circuit, permeates the sample, and (usually) causes a precessing magnetization, which changes the magnetic flux in the solenoid over time, inducing a current, which can be detected. Since both the input pulse and output signal traverse the same circuit path, the power amplifier and signal preamplifier must be properly impedance matched. A crossed pair of diodes ground the high RF voltages that arrive with the transmitter is on, while picking out the weaker resultant signal when received.

The signal output from the probe is amplified and then input to the phase detector and mixed with the reference signal. The resulting signal, comprised of "beats" between the two very close frequencies is displayed on the oscilloscope, which triggers on the original input RF pulses.

B. Execution

C. Determination of Pulse Widths

We first determined the pulse widths in time corresponding to π and $\pi/2$-pulses. Originally, we set the RF pulse generator to a specific amplitude setting: $V_{\rm pp} = 2.00$ V and then varied the delay setting on the DPP (for a single pulse sequence) until we minimized the free induction decay (FID) signal following the pulse. This method yielded a value of 48 μs for the π-pulse, which was cut in half to determine the $\pi/2$-pulse width. However, realizing that we had finer control over the amplitude of the RF field with the pulse generator, we instead tuned the digital pulse programmer to generate a 50 μs pulse width and minimized the FID signal by varying V_{pp} to achieve the π-pulse.

D. Measurement of T_1

We utilized the three-pulse method pioneered by I. Chuang and R. Sarpeshkar to measure T_1 for four different aqueous glycerine solutions: 88% to 100% glycerine by weight in steps of 4%. An example of raw data for this pulse sequence is shown in figure 3.

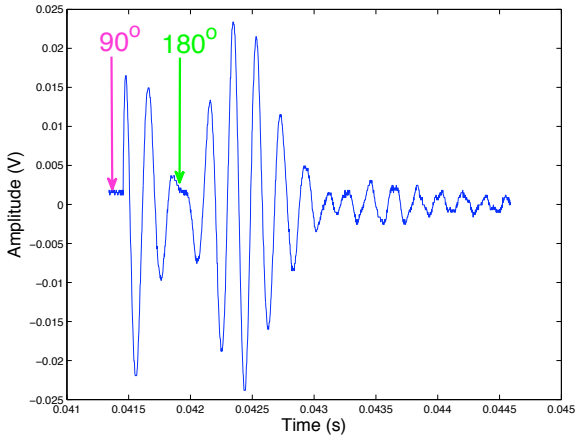

FIG. 3: Raw data for the calculation of T_1 using the three-pulse sequence. Data is shown for an aqueous glycerine solution. Figure created by S. Campbell

We varied τ differently for each compound, such that we took about 10 data points for each solution over a reasonable range, depending on the expected value of T_1 for the particular sample.

E. Measurement of T_2

The Carr-Purcell pulse sequence is described in detail in the Appendix. We used this sequence, which can be described as $\pi/2, \tau, [\pi, 2\tau]^N$, on the same aqueous glycerine solutions, keeping τ fixed at 5 ms, while capturing the entire spin echo train. We used the oscilloscope's screen capture capability to read out a bitmap image, like in figure 4 of the signals, from which we later extracted the signal amplitudes. Additionally, we took measurements of three different concentrations of paramagnetic ions, 10^{16}, 10^{17}, and 10^{18} Fe^{+++} ions/cc, but some of the data was obscured due to a mistake in the readout process.

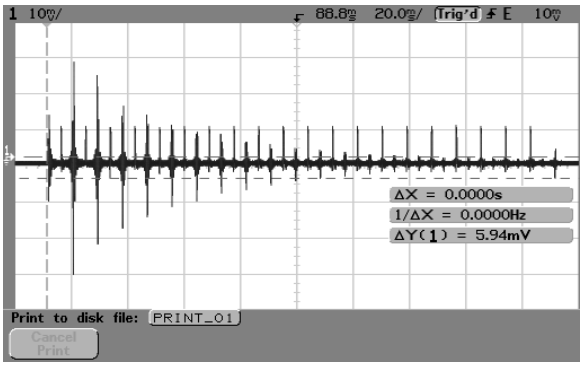

FIG. 4: An oscilloscope screen shot displaying a Carr-Purcell train for an aqueous glycerine solution.

IV. DATA AND ERROR ANALYSIS

Data reduction and analysis was done using MATLAB with linear and nonlinear fit scripts provided by the Junior Lab staff.

A. Systematic and Statistical Error Analysis

Sources of the systematic error include the oscilloscope's technical resolving limit, the pixel resolution of the bitmap images for T_2 measurements, the non-uniformity of the magnetic field, and the general variance in signal amplitude. These errors, where appropriate, were added in quadrature to calculate error bars for the plots in the following sections.

The oscilloscope precision was taken to be $\pm$ 0.6 mV [3]. In addition, by taking multiple screen shots of a spin echo from a sample of 88% glycerine subjected to a $\pi/2, \pi$ pulse sequence and observing the variance in these, we determined the statistical fluctuations to be $\pm$ 11.25% of the voltage amplitude (the standard deviation of the five measurements). Finally, we estimated the pixel resolution of the bitmap screen shots to be $\pm$ 2 pixels, corresponding to $\pm$ 6.5 mV.

B. Static Magnetic Field and Magnetic Moments

We took measurements of the static magnetic field, the precession (Larmor) frequency of hydrogen and fluorine, and the magnetic moments of hydrogen and fluorine using glycerine and hexafluorobenzene, respectively.

By minimizing the FID which occurs in coincidence with resonance, we found the precession frequencies for hydrogen and fluorine to be $\nu_H = 7.52203 \pm 0.0002$ MHz and $\nu_F = 7.52224 \pm 0.00005$ MHz. Using the relation found in equation 3, it follows that,

$$\mu_H = (1.4099 \pm .0048) \times 10^{-26} \text{ Joules/Tesla}$$
$$\mu_F = (1.4094 \pm .0056) \times 10^{-26} \text{ Joules/Tesla.}$$

From these results we determined of the strength of the magnetic field,

$$B_0 = 1768 \pm 1 \text{ Gauss.}$$

C. Effect of Viscosity on Relaxation Times

For both relaxation times, we fit exponentials to the data as functions of the parameter τ, the delay between pulses.

To determine spin-lattice relaxation time, T_1, the three-pulse method measures the proportion of longitudinal magnetization recovered by time τ by creating a spin echo proportional to the recovered population. Thus, we expect an exponentially increasing amplitude for increasing delay between pulses, [4]

$$M(\tau) = A(1 - 2e^{-\tau/T_1}). \quad (7)$$

We performed a least-squares non-linear fit to equation 7 for each of the aqueous glycerine solutions. Contrastingly, for spin-spin relaxation time, we expect an exponentially decreasing relationship, with time constant T_2, when we measure the spin echoes created by the Carr-Purcell method. Therefore, we fit to a different exponential :

$$M(n2\tau) = Ae^{-n2\tau/T_2}. \quad (8)$$

where $M(n2\tau)$ represents the amplitude of the n^{th} spin echo which occurs at time $n2\tau$

In the non-linear fit to extract T_2, comparing equations A.1 (from the Appendix) and 8, we ignored an exponential term that is third order in τ. The lack of or inaccessibility of information regarding the diffusion coefficients for our samples and the inhomogeneity of the magnetic field made including this term unfeasible. This may have contributed to the apparent structure in the residuals seen in figure 5. However, it is encouraging that the reduced chi-square, $\chi^2 = 0.081$, is small, indicating a good least-squares fit.

There were more difficulties in deriving the spin-lattice relaxation time. Each of the four data sets had fits with discernable structure in the residuals. We conclude that there must be other effects that are not accounted for in formula 7.

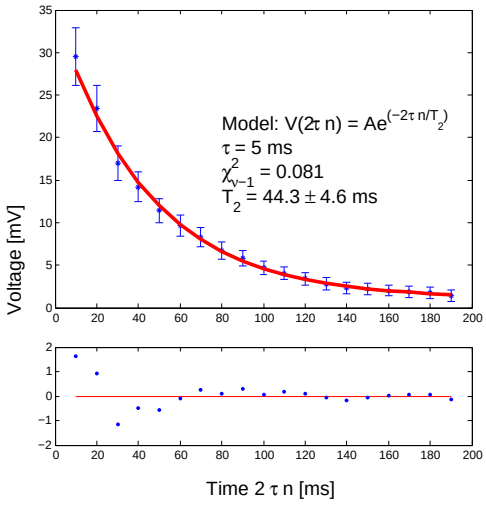

FIG. 5: The results of the exponential decay fit for 92% glycerine. Note the apparent structure in the residuals and the $\chi^2_R = 0.081$.

% Glycerine by weight	Viscosity [Cp/mPas]	T_1 [ms]	T_2 [ms]
88	175	20.29 ± 1.04	80.16 ± 4.15
92	310	18.12 ± 1.17	54.74 ± 2.95
96	624	19.09 ± 0.60	33.21 ± 2.40
100	1410	8.90 ± 0.60	19.93 ± 2.01

TABLE I: This table displays the extracted time constant from the exponential fits to the eight data sets. Errors are a result of propagating the voltage errors and the $\chi^2_R = 0.067$.

The final results for our measurements of T_1 and T_2 are tabulated in table IV C. Viscosities were read off of or extrapolated from a reference table in [4]. A log-log plot of T_2 versus viscosity of solution is shown in figure 6.

Though we also took data for different paramagnetic ion concentrations, the data did not follow the trend we expected from the literature [5]. More fundamentally, the spin echo amplitudes for a single concentration, did not follow the exponential decay expected, making an exponential fit procedure highly suspect. This may due to the fact that we used $\tau = 5$ ms, when we expected only slightly larger T_2 values. This means we could only see a small portion of the decay and due to the large uncertainties inherent in the measurement, we could not fit the data successfully.

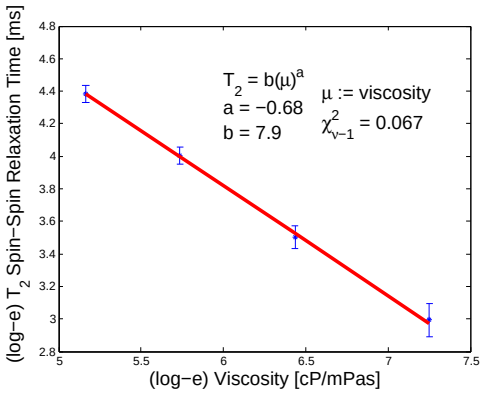

FIG. 6: A log-log plot in base e displaying the relationship between the spin-spin relaxation constant and the viscosity of the sample.

V. CONCLUSIONS

Our findings for the dependence on viscosity of the spin-spin relaxation time T_2 are in good agreement with Bloembergen, *et al.* Even the slope of the line, which for them is approximately $-\frac{2}{3}$ while ours is -0.68 ± 0.05, is reasonably consistent. [5]. This indicates the power law relationship between viscosity and T_2 that we measured is very similar to established findings.

In addition to these findings, our measured magnetic moment of hydrogen is in good agreement with the accepted value, however the value we measured for fluorine was substantially different and in fact, very close to the value we observed in hydrogen.

The inversion of the expected relationship between T_1 and T_2, i.e. that $T_1 \gtrsim T_2$, may indicate that T_1 is actually greater than the values we report in IV C.

The effects delineated here, especially the residuals apparent in the fits, warrant further investigation. Future research will hopefully yield better measurements of T_1, a good estimation of the magnetic field variation, and overall better agreement with the theory.

Appendix: Spin Echoes and Carr-Purcell

Hahn's discovery of spin echoes invigorated the study of NMR, by demonstrating that the magnetic field inhomogeneity may be disregarded in the measurement of T_2. One way to generate a spin echo is by applying two pulses of fixed widths and delay, near Larmor resonance $\omega \approx \omega_0$. This is known as a $\pi/2, \tau, \pi$ pulse sequence. The following discussion ignores T_1 and T_2 effects.

A $\pi/2$-pulse refers to a pulse that lasts a time $t_{\pi/2}$ such that $\omega t_{\pi/2} = \gamma B_0 t_{\pi/2} = \pi/2$ and a π-pulse has double duration. Suppose the transverse field, in the $+x$-direction is applied for a time $t_{\pi/2}$, then the magnetization vector of the sample (initially pointing in the $+z$-direction), is rotated down into the x-y plane, say, along the $-y$-direction. By waiting a small time τ, the magnetization precesses about the static field, staying in the transverse plane and rotating by an angle $\theta = \gamma \Delta B \tau$, where $\Delta B = B_1 - B_0$.

A π-pulse applied at time τ (B_1 again in the $+x$-direction) reverses the phases of the magnetization of individual particle, that is, those spins that were ahead by a certain phase, now lag by that same phase. Since the "advance" of the spins is still in the same direction, after a time τ, the spins will have completely re cohered, restoring the state that occured directly following the first $\pi/2$-pulse, except the magnetization is in the $+y$-direction. This means that the same FID signal is induced as if the $\pi/2$-pulse just happened. Additionally the form of the signal just before time 2τ is the exact mirror image of the decay afterwards.

We can account for T_1 and T_2 effects by noting that during the first τ interval, the spin vector will rise exponentially (with time constant T_1) back up to the z-axis. Thus, the size of the magnetization in the x-y plane at time τ^+ is smaller by that amount. During the next τ interval, the component of magnetization in the x-y plane will continue to decay with time constant T_2 and as a result, we see the size of magnetization producing the echo signal will obey [6]

$$M(2\tau) = M_0 e^{-2\tau/T_2}$$

Further, Carr and Purcell showed that diffusion leads to a decay of the spin echo amplitude M, given by

$$\begin{aligned} M(2\tau) &= M_0 \exp\left[-D\gamma^2 \frac{\partial B}{\partial z}^2 \frac{2}{3}\tau^3\right] \exp\left(-2\tau/T_2\right) \\ &\equiv M_0 \alpha \end{aligned}$$

where we have assumed $B_1 - B_0 = z\left(\frac{\partial B}{\partial z}\right)$. If we apply yet another π-pulse 2τ after the first, we see that the next spin echo will be attenuated again by the same factor α. Proceeding by induction, we see that if we apply a "Carr-Purcell" pulse sequence: $\pi/2, \tau, [\pi, 2\tau]^N$, then we see a train of spin echoes, such that the amplitude of the n^{th} spin echo obeys:

$$\begin{aligned} M(n2\tau) &= M_0 \alpha^n \\ &= M_0 \exp\left[-\gamma \frac{\partial B}{\partial z}^2 D \frac{1}{3}(n2\tau)\tau^2\right] \\ &\quad \times \exp\left(-n2\tau/T_2\right) \end{aligned} \tag{A.1}$$

This formula makes it possible to measure T_2 as in this experiment without worrying too much about the diffusion and inhomogeneity terms.

Acknowledgments

The author acknowledges Sara Campbell's equal partnership in the preparation and execution of this exper-

iment. The author also thanks Professor David Litster, Daniel Furse, Regina Yopak, and Dr. Emily Edwards for their help and input.

---

[1] A. Melissinos and J. Napolitano. *Experiments in Modern Physics*. Elsevier Science, second edition, 2003.
[2] J. Negele. 8.05 Quantum Physics II. lecture notes, 2008.
[3] Agilent oscilooscopes user's guide. http://cp.linterature.agilent.com/litweb/pdf/54622-97036.pdf.
[4] MIT Department of Physics. Pulsed nmr: Spin echoes. Lab Guide, 2008.
[5] R. P. N. Bloembergen and E. M. Purcell. *Phys. Rev.*, 73, 1947.
[6] C. P. Slichter. *Principles of Magnetic Resonance*. Springer-Verlag, 1989.